Stability of electrons and X-rays generated in a pyroelectric accelerator.

M. Ali[1*], P. Karataev[1], A. Kubankin[2,3], A. Oleinik[2]

[1]John Adams Institute at Royal Holloway, University of London, Egham, Surrey, TW20 0EX, UK
[2]Belgorod National Research University, Pobedy St. 85, 308015 Belgorod, Russia
[3]P.N. Lebedev Physical Institute of the Russian Academy of Sciences, Moscow 119991, Russia

Conventional X-ray sources are far too bulky and require a high-power DC voltage. The pyroelectric X-ray generator technology has enabled us to develop portable, low-power X-ray sources for use in materials analysis, imaging, and other applications. Changing the temperature of single crystal lithium tantalate (LiTaO3) at moderate vacuum conditions gives an attractive possibility to generate and accelerate electron up to 100 keV. The electrons are ejected either from the crystal or from the target (depending on polarity). The electrons then generate X-rays via bremsstrahlung and characteristic X-ray emission processes. The aim of this experimental investigation is to explore the interesting feature of the pyroelectric accelerator that generates a monoenergetic electron flux with a stable value of peak energy for a long time. Here we present studies of features of electron flux in pyroelectric accelerator depending on the pressure of residual gas and the distance between the crystal and the target-collimator. We examine the correlation between monoenergetic electron production and avalanche discharge. We also studied outgassing from some accelerator components. The pyroelectric X-ray generator technology is currently being developed is a reliable, compact, stable, and reproducible X-ray source with controllable parameters, which does not require a high-power DC voltage or the use of hazardous (radioactive) materials.

Introduction

It is well known that pyroelectric crystals can convert the thermal gradient into electrical energy. A pyroelectric material possesses a spontaneous dipole moment when there is no applied electric field [1]. In thermal equilibrium, an induced surface charge is completely balanced. A distinctive feature of pyroelectric crystals is that the spontaneous polarization of the crystal changes dramatically in response to a temperature change. In vacuum conditions, the spontaneous polarized charges appear on the surfaces of the crystal due to temperature change of the crystal [2]. This is called the pyroelectric effect.

During temperature change in low vacuum conditions, the bulk polarization changes, leaving uncompensated surface charges that generate a high electric field with a strength of about 10^5-10^6 V/cm [3]. The sign of the field depends on the orientation of the crystal and whether the crystal is being heated or cooled. This phenomenon is possible in LiTaO3 at moderate vacuum conditions of less than 10^{-2} Torr to avoid any field shielding. The electric field is high enough to initiate field electron emission and impact ionization of the residual gas molecules and the surroundings [4, 5, 6, 7]. The electrons and positive ions obtain energy in the electric field between the crystal and the target and interact with matter [8, 9, 10, 11], generating characteristic X-ray photons and bremsstrahlung. The characteristic X-ray lines allow us to identify the sample material, which can be directly applied for its element analysis [12, 13, 14]. The maximum energy of the bremsstrahlung is called the endpoint energy, which corresponds to the maximum potential developed along the crystal.

Conventional X-ray sources are far too bulky, cannot produce small enough beams, and require large DC voltage power supplies. The pyroelectric X-ray generator is compact with low power consumption, which allows us to complement the high-voltage conventional X-ray tubes. Of cause, the X-ray intensity is low, but detectable, enabling quick test measurements on field trip research or at difficult to reach locations, e.g. the space station.

The first step towards a practical realization of this technology has been made by the Amptek company, who developed the first compact X-ray source based on pyroelectric effect [15]. However, unstable X-ray emission, and lack of reproducibility of the X-ray spectra prevents the widespread of pyroelectric sources for practical application.

The properties of the pyroelectric crystal must be considered to understand the progress of pyroelectric crystal as a source of radiation. Inadequate understanding of the processes between the target the crystal is linked to the unstable generation of particles. In this paper, we review the fundamental issue of charge particle generation in pyroelectric accelerator. The impact of distance between the crystal and target on generation of stable X-rays were investigated step by step.

The outgassing effect was investigated as well. It occurs via several processes including vaporisation (from the cooling system) and release of molecules bound at crystal assembly can contribute to the background current as an electron source.

* Corresponding author: Majid.Ali.2021@live.rhul.ac.uk

Experimental setup

A schematic sketch of the experimental setup is shown in Figure 1. The pyroelectric crystal assembly consists of a $LiTaO_3$ parallelepiped (20mm x 20mm x 10mm) shape single crystal attached to Peltier element. The foil was glued between the crystal and the Peltier element to provide a good electrical contact and to measure the current. Also, the foil attached to the crystal and Peltier element were separated by a mylar foil. The whole assembly was set on the heat sink in a vacuum chamber. The top and bottom surfaces of the crystal were polished. The Peltier element was used to change the temperature of the crystal. It was powered by the arbitrary waveform generator TGA12104 (amplified by the waveform amplifier Accel TS250). When the crystal was heated, its top z^- surface was charged positively. This results in the acceleration of electrons from the target to the crystal, causing characteristic X-rays from the crystal to be observed (see, for instance, Fig. 2). During cooling, the crystal was re-polarized. The top z^- surface then gained negative charge, causing it to emit electrons toward a grounded target.

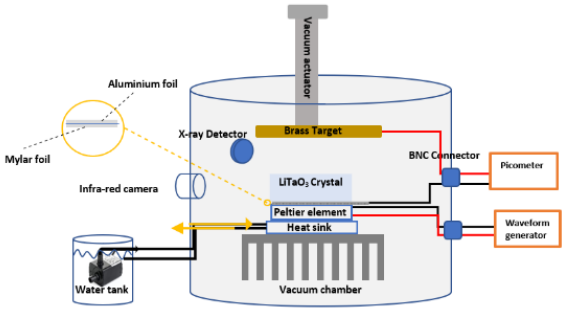

Figure 1. The scheme of experimental setup in vacuum conditions.

An infrared camera Flir E30 was focused on the pyroelectric sample via a 0.5 mm thick infra-red transparent diamond window, and enabled contactless measurement of the crystal temperature. The measurement range of the camera was from -200C^0 to 1500 C^0. The temperature oscillations were recorded near the top and the bottom surfaces of the LiTaO3 crystal throughout the operation. A brass plate (target) was mounted on a vacuum actuator, allowing to change the distance between the target and the pyroelectric crystal, which was connected to a Picoammeter (Keithley In-struments Inc., 6485) to measure the electron current from the crystal surface to the target. A special protection circuit consisted of a resistor and two diodes integrated to prevent overload conditions at a breakdown. The current data monitoring and recording are implemented by the LabVIEW program. The gap between the top surface of the pyroelectric crystal and the target is represented as a capacitor.

All the experiments were performed at a low-pressure range as X-ray counts are affected by the fluctuation of pressure. The semiconductor Amptek Cd-Te XR-100T X ray detector was mounted on a separate vacuum chamber viewport to measure the X-ray spectrum radiation from both the target and top surface of the crystal. This detector was mounted in such a way that the entrance window of the detector was at almost the same distance from the top surface of the pyroelectric sample and the target. The endpoint energy of these spectra was used to estimate the acceleration potential.

A water-cooling system was attached to the heat sink to extract residual heat from the Peltier element. A water tank was placed outside the vacuum chamber and a submersible pump was connected to the heat sink by plastic tubes to circulate water through the sink. The temperature of the water was measured by a thermocouple and was kept constant throughout the measurement phase by adding ice into the water. This to ensured that the same amount of extraction took place cycle by cycle through the experiment. The experimental results show that a stable oscillation of temperature is required for stable particle generation. The vacuum chamber was connected to a vacuum pump via a short, flexible pipe. The system included the rotary vane fore-vacuum pump and the turbomolecular pump. The fore-vacuum pump implemented the initial pumping of the vacuum chamber through the turbomolecular one. When the pressure reached about 0.15 Torr, the turbomolecular pump started to obtain the lowest level of pressure to be 0.5mTorr.

It is necessary to provide a residual gas pressure around the pyroelectric sample of about 1.0 mTorr. So, to lower the pressure level in the chamber, it faces obstacles like vaporisation from the cooling system and the release of molecules bound at crystal assembly into the chamber. Also, the vacuum gauge can contribute to the background current as an electron source. The additional valve gate is used to cut off the gauge electrons from the main vacuum chamber. It allows the elimination of additional particle flow. In our case, vaporisations from the cooling system (thermal evaporation), adhesive materials (used in crystal and target assembly), and cables used inside the camber are the most common sources of outgassing. Therefore, it is important to have a good understanding of how different techniques can be used to reduce all possible sources of outgassing. The appropriate combination of material selection, cleaning, and preparation, outgassing rates can be reduced. Therefore, the choice of materials for a vacuum system and the procedures followed before an experiment are critical to ensure the success and reliability of the experiment. Here's an overview of the points that have been addressed in our research and should be addressed by anyone attempting to reproduce the system:

- Vacuum chamber Material: Vacuum compatibility. The chamber material should be

compatible with the vacuum level, pressure, and the substances involved in the experiment. Stainless steel, aluminium, or glass have been chosen in our case due to their low outgassing rates, chemical resistance, and non-magnetic nature.

- Target material: The choice of target material depends on the experiment's objectives. In our case they were made of solid materials compatible with the vacuum conditions. Liquid or gas targets must be sealed in a vacuum compatible container.
- Epoxy glue: Epoxy is often used for sealing crystal and Peltier element inside vacuum chamber due to its low outgassing properties. Special low outgassing epoxy (Conductive Epoxy CW2400, CircuitWorks Solutions) has been chosen in our experiment to minimize contamination of the vacuum environment.
- Cables: Cables inside the vacuum chamber are made of materials with low outgassing rates. Materials like Kapton or PTFE are common electric isolator choices.
- Windows: Dimond window is used for optical access to measure the temperature of the crystal, materials like specific types of glass is chosen for their transparency in the desired wavelength range and resistance to vacuum conditions.
- Cleaning: Thorough cleaning is essential to remove contaminants that could compromise the vacuum environment. Solvents and cleaning methods compatible with the chosen materials should be used. We used isopropanol for this purpose.
- Leak testing: Before an experiment, the vacuum system was vacuum tested to ensure there are no unwanted leaks. The vacuum of 10^{-6} Torr was easily achieved.
- Pumping: The chamber is often purged with clean gases and then pumped down to the desired vacuum level. To control the vacuum we used a fore vacuum pump (Edwards RV3, Edwards Vacuum) to achieve vacuum level of 0.5 Torr and a turbomolecular pump (Pfeiffer Vacuum Balzers, TPH-170) in a chain to reach 0.1 mTorr level. The vacuum level was controlled by a vacuum meter (Kurt J. Lesker, KJCL Cold Cathode Series CCPG-H2-1). A vacuum gate valve was used to degrade the vacuum, if necessary, to keep it within a selected range of 0.5 – 1.5 mTorr.
- Environmental control: The experiment environment should be controlled for temperature, humidity, and other factors depending on the experiment's requirements to minimize interference and ensure accurate results. The cooling water temperature was controlled by a thermocouple thermometer.
- Monitoring and maintenance: Continuous monitoring and maintenance of the vacuum system was conducted to detect and rectify any issues that may arise during an experiment.

The choice of materials and the pre-experiment procedures should be tailored to the specific needs and constraints of the experiment. This involves a balance between the experimental requirements, material compatibility, considerations to ensure the experiment's success and data integrity.

The two schemes to generate X-ray at positive and negative polarities are illustrated in Figure *2*. Two different possibilities can be realized for X-rays generation, when a grounded target is placed in front of the polar surface of the crystal in a vacuum. If the pyroelectric crystal surface is negatively charged - Figure 2 (a), the electron emissions were initiated from the vicinity of the crystal surface and accelerated to the grounded target, producing bremsstrahlung and characteristic X-rays of the constituent atom of the target. When positive charge was accumulated at the crystal surface - Figure 2 (b), the electrons were emitted from the target, gaining energy in the gap and generating X-rays from the constituent atom of the crystal.

It should be noted that the ions of the residual gas are also accelerated in the opposite direction relative to the electron propagation, but the ions' X-ray yield is substantially smaller in comparison with the yield produced by the electrons. Several other geometries can be realized to develop pyroelectric X-ray sources [9, 16, 17].

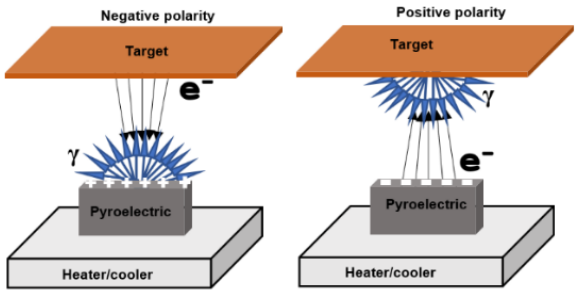

Figure 2.(a) Generation of electrons at positive polarity: (b) Generation of electrons at negative polarity.

Results and analysis

The influence of the gap between the target and the crystal on particle generation

It was confirmed experimentally in our previous measurement that the generation of the X- rays depended on the atmospheric pressure [18, 19]. At high pressure, X-ray generation is negligible. We found that at a specific

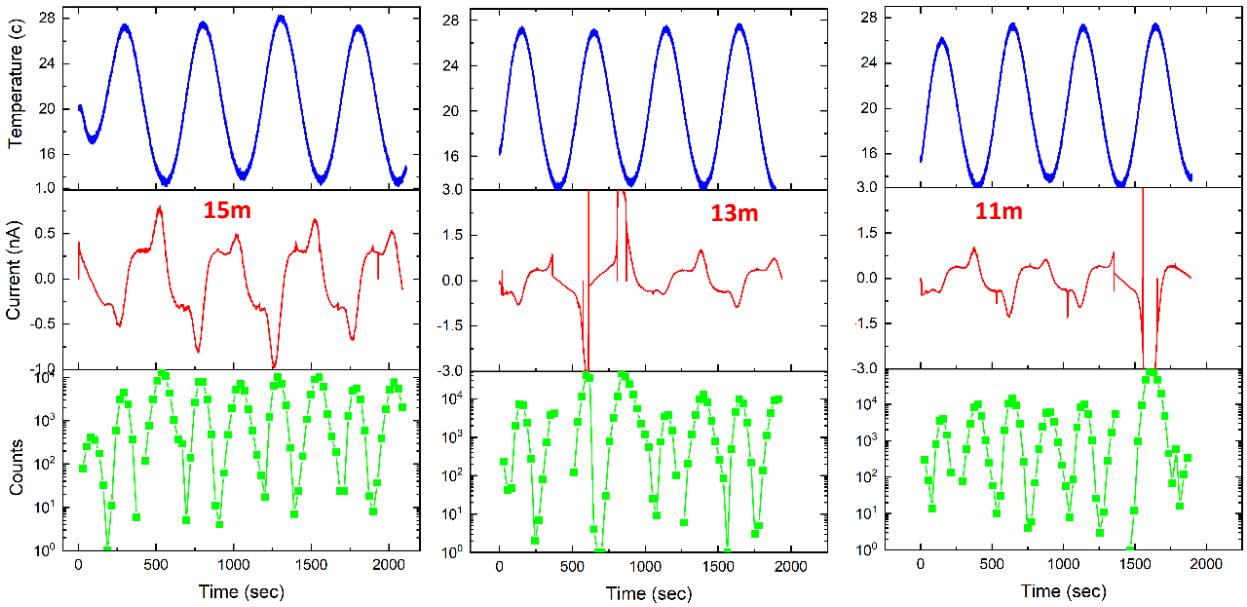

Figure 3.The measurement results during periodic temperature variation at the frequency of 2 mHz and pressure 2 mTorr at 11,13, and 15 mm gap between the target and the crystal.

atmospheric pressure at which maximum X-rays were generated depended on the experimental arrangements of the target with respect to the pyroelectric crystal. We studied the impact of the distance between the target and the crystal on generation of stable X-rays.

The distance between the target and the crystal varied from 3mm to 21mm with a step of 2mm. The frequency, the amplitude of temperature, and the pressure were kept constant at 2mHz, 150mVrms, and 01-02 mTorr respectively.

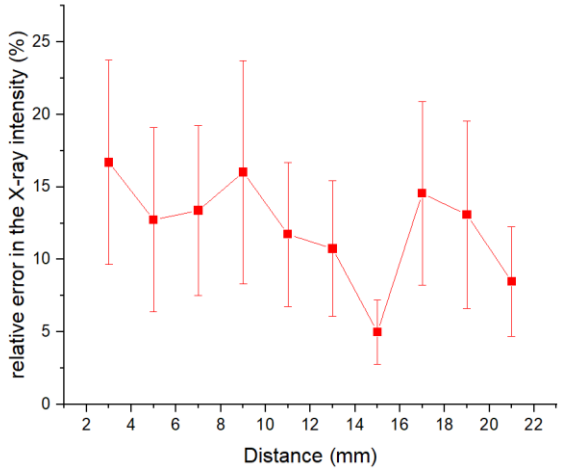

Figure 4. The relative error in the X-ray intensity is plotted against the distance between the target and the crystal. The error bars represent the uncertainty deviation from average.

Examples of experimental data plotted over the four full thermal cycles for 11 mm, 13 mm, and 15 mm distance are shown in Figure 3. The data collected over four full thermal cycles demonstrate clear reproducibility in the intensity of X-rays cycle by cycle for various distances. To analyse the uncertainty in experimental data, we calculated the relative errors in X-ray intensity against the distance, which is a measure of the uncertainty of the X-ray intensity of each thermal cycle at a specific distance. The relative errors in the four thermal cycles were plotted for each distance, and each point in Figure 4 represents these finding.

This analysis demonstrated that the stability of X-rays generation at the distance of 15 mm is less than 5 %, which is the minimum uncertainty among all the distances. This suggests that the X-ray generation at 15 mm distance is reproducible at almost same intensity throughout the experiment. The relative error is measured above 10 % for the distances below and above 15 mm, which is much higher, and indicates that the X-ray emission stability cycle by cycle is a function of the distance. Furthermore, the most unstable and poor X-ray generation was observed at 3 mm distance, with a relative error of 17 %. This study concluded that the optimal distance to generate stable particles and X-ray was 15 mm at 2 mHz frequency of temperature variation and pressure of 1-2 mTorr.

In pyrolectric accelerator, the crystal becomes electrically charged and generates focusing forces for the electron beam [20]. We believe that at 15 mm distance, the electrons focus on the target, and as a result, the X-ray generation process is reproducible cycle by cycle, while for the other distances, the electrons began to diverge, and,

consequently, the X-ray flux varies from cycle to cycle. It will require further study we plan to investigate and confirm the focal distance for the electron beam.

Figure 5 presents a comparison of the current oscillation amplitude at different distances between the target and the crystal at 2 mHz frequency of temperature variation. In Figure 3, the current curve consists of the smooth sinusoidal wave and the breakdown spikes that interrupt the wave. The spikes manifest at distance of 11 mm and 13 mm. However, there are no X-ray photons generated. The absence of the X-ray generation that those spikes are electrical breakdowns between the crystal and the ground. It is not a breakdown between the crystal and the target. Numerous spikes indicate that short breakdown discharges occur from time to time. The exact nature of these discharges requires additional studies. One of the possible explanation is the spontaneous crystallographic plane displacements inside the crystal due to imperfections of the crystal lattice.

The sharp spikes were extracted from the measured data and were not analysed. The current amplitude reduces with the increase of distance between the target and the crystal.

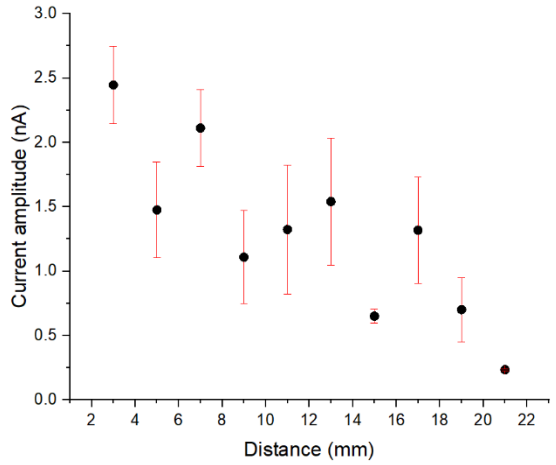

Figure 5. The comparison of current oscillation amplitude against the distance between the crystal and the target.

First, we note a very strong dependence of the current curve on the target to crystal distance. The current amplitude generally decreases with the distance increase. When the distance is larger the electric field strength is weaker. So, the field emission results in a smaller number of electrons ejected from the cathode. Therefore, the current amplitude decreases. On the other hand, at larger distance the amount of residual gas is larger, so the number of particles reaching the anode is smaller as well.

Characterization of the avalanche discharge in the gap between crystal and the target.

Two cases of positive and negative polarities of endpoint energy versus current are plotted in Figure 6. The red graph presents a negative polarity half-cycle, and the blue graph present a positive polarity half-cycle. The pressure in both cases ranged from 0.5-0.75 mTorr, and the temperature oscillation frequency was 0.5 mHz. The red and blue circles show the experimental points of the endpoint energy. Grey arrows with numbers represent the direction of dependence over time and indicate the different phases of the experiment. Both curves represent hysteresis loops of the avalanche process between the crystal and the target discussed in [19] in details. The difference of Figure 6 from [19] is that here both slow current wave and the avalanche peak are used. The structure of the curve significantly differs for each polarity. At the positive polarity, electrons are ejected from the surface of the target by a positive potential in the gap, while at the negative polarity, electrons are ejected from the vicinity of the polar surface of the crystal.

To have a better analysis of these observations, it is interesting to compare the variation of the electric field strength as a function of the discharge current with the typical voltage–current (V–I) characteristic of a discharge between electrodes under ac voltage. Figure 6 illustrates an equivalent of the V-I dependence characterizing the avalanche discharge process in the pyroelectric accelerator setup, this comparison is meaningful because in our experiment the current and voltage variations are slow corresponding to the sensitivity of our detector.

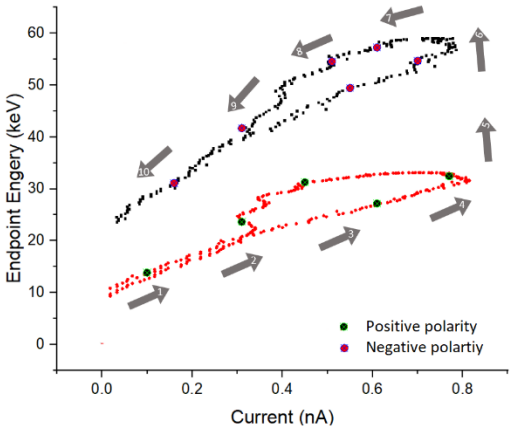

Figure 6. The red curve presents a negative polarity half-cycle, and the blue curve presents a positive polarity half-cycle. The pressure ranged from 0.5 -0.75 mTorr, and the temperature oscillation frequency was 0.5 mHz.

As the temperature starts to change, an electric field is generated between the crystal and target, leading to field electron emission. Initially, the number of electrons grows, but the generation of X-rays is not observed at this point

because the electron energy is not high enough to initiate impact ionization. The first experimental point proposed that the electrons, which gained sufficient energy, initiate the impact ionization of the target, this would lead to the current increase, which is associated with an ionization increase and the appearance of the characteristic and the higher energy bremsstrahlung X-ray photons. The voltage stabilizes while the current is still increasing. Because the temperature gradient reduces slowly, the voltage in the gap between the crystal and the target reduces as well leading to a slow decrease in the voltage potential. As a result, the endpoint energy and the current in the circuit decrease too. When the current changes its polarity, the process repeats, the current's direction reverses. The direction of the electron flow is also indicated by the characteristic X-ray spectra, with X-rays coming from the target at negative polarity and from the crystal at positive polarity. The discharge process is different at different polarities due to the different work function of the crystal and the metal. Pyroelectric crystal is a dielectric material, which is more complicated because of the population of the internal electron energy states does not obey Fermi distribution, and there is an internal electric field due to the polarization of the material. It is believed that the work function of the crystal is smaller than the metal, Therefore, the emission of electrons from the crystal begins at a lower electric field strength. However, amplifying the electron flow by impact ionization of molecules is not possible at low pressure. The standard avalanche Townsend discharge does not fit, as shown by our analysis of V-I dependence [21].

Investingation of outgassing process in pyroelectric accelerator

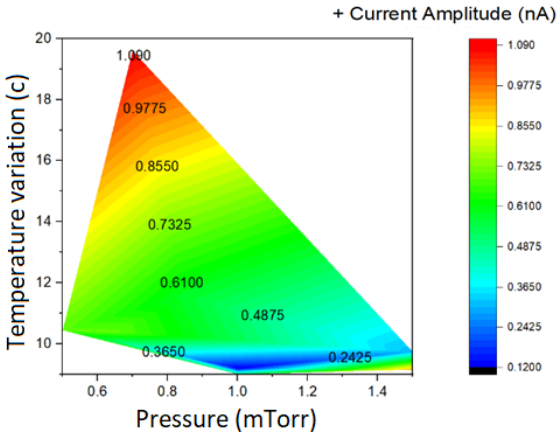

Figure 7. The dependence of the current amplitude as a function of the peak-to-peak amplitude of temperature oscillations at the top surface of the pyroelectric sample and pressure (positive polarity).

To investigate the electron avalanche at low pressure, the experiments were repeated at different pressure ranges from 0.5 mTorr to 1.5 mTorr. The measured parameters during periodic temperature variation with frequency of 0.5 mHz and the pressure region of 0.5–1.5 mTorr were collected over four full thermal cycles, and an average value of four cycles of current amplitude of positive polarity was plotted in Figure 7.

The value of the current amplitude was insignificantly changed by the pressure. It is worth noting that the amplitude becomes higher at pressures lower than 0.9 mTorr. At above 1 mTorr pressure, the current amplitude was observed to be below 0.73 nA, apart from the current amplitude of about 0.8 nA observed at 1.4 mTorr pressure. This is because of charge multiplication due to impact ionization at the crystal or target. At low pressure, the current amplitude generally decreases due to the low density of residual gas molecules, but in this case, at a pressure range of 0.7–0.8 mTorr, the current amplitude is at its maximum (1.09 nA). It was likely that the epoxy used in crystal assembly and the cooling system were outgassing into the system.

Outgassing is defined as the release of a gas that has been trapped, or absorbed, in a material. This means that all surfaces, no matter what material is under consideration, outgas under high vacuum. The air bubbles can be trapped in the assembly. These air bubbles can cause defects such as cavities in the components. These cavities give rise to electrical breakdowns. Gas molecules can be ionized by the striking electron. The energetic ions can strike the target and contribute to the collector current. The release of gases and vapours from the components inside the vacuum system contributes to the current amplitude [22, 23]. In the case of a pyroelectric accelerator, the outgassing occurs due to the release of air that has been trapped in the pyroelectric assembly (between the Peltier and the crystal).

Outgassing due to thermal evaporation was also investigated by changing the temperature variation at a fixed pressure level (0.5 mTorr), as shown in Figure 8.

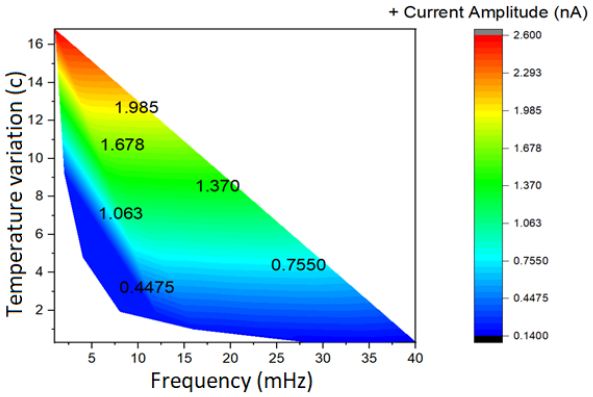

Figure 8. The dependence of the peak-to-peak amplitude of temperature oscillations at the top surface of the pyroelectric sample and frequency on current amplitude (positive polarity).

It was observed that the current amplitude is higher at low frequency. In fact, here outgassing was due to thermal evaporation comes into effect. The rate of outgassing increases at higher temperatures; decreasing the frequency leads to a higher variation temperature that causes electrical breakdown due to outgassing because of thermal evaporation. Vaporisation from the cooling system was also considered to contribute to the discharge process. Thermal evaporation and adhesive materials were the most common sources of outgassing.

Conclusion

Sudden interruptions of X-ray generation in pyroelectric sources are the main problem of stability for application of this technology in the broad field. Periodically varying the temperature of LiTaO3 crystal with proper residual heat extraction enabled us to generate a stable particles stream and a quasi-continuous X-ray beam. We investigated the impact of target-to-crystal distance on stable particle generation, establishing that an optimal distance is required for a specific frequency and pressure range in order to generate reproducible particle streams.

These finding support the argument that the electric field should allow charged particles to acquire enough energy to reach the target or crystal and initiate a discharge. If the distance is too short, the electron reaches the anode without colliding with residual gas molecules. If the distance is too long the electron gives its energy in a series of non-ionizing collisions.

It is difficult to assess the outgassing contribution, but it is clear from the above results that outgassing contributes to the current amplitude and alter the collected current. It is concluded that the rate of outgassing increases at low pressure. The lower the pressure, the more outgassing occurs.

The bottom line is that for optimal pyroelectric accelerator operation a multiparameter optimization is needed. We shall continue investigating stability issues and optimal crystal assembly for efficient and reproducible particle production.

The continued study of pyroelectric sources proposes that the use of pyroelectricity for X-ray generation has great advantages. Soon, more portable X-ray devices will be available, and these new designs will offer stable and reproducible sources of X-rays with controllable parameters. These X-ray sources are safer and easier to operate, since they required only 12 Volts instead of kVs.

Acknowledgement

The work was supported by the Science and Technology Facilities Council via John Adams Institute for Accelerator Science at Royal Holloway, University of London (Grant Ref. No. ST/V001620/1.

The work of AK and AO was financially supported by a Program of the Ministry of Education and Science of the Russian Federation for higher education establishments, Project No. FZWG-2020-0032 (2019-1569).

References

[1] K. K. Wong, "Properties of lithium niobate," INSPEC [Orig.-Prod.], LONDON, 2002.

[2] J. D. Brownridge and S. M. Shafroth, "Electron and positive ion beams and x-rays produced by heated and cooled pyroelectric crystals such as LiNbO3 and LiTaO3 in dilute gases:phenomenology and applications," *Nova Science Publishers,* pp. 57-94, 2005.

[3] B. Rosenblum. et. al., "Thermally Stimulated Field Emission from Pyroelectric LiNbO3," *Appl. Phys. Lett,* pp. 17-22, 1974.

[4] J. D. Brownridge, et. al., "Observation of multiple nearly monoenergetic electron production by pyroelectric crystals in ambient gas," *Appl. Phys. Lett.,* pp. 1158-1159, 2001.

[5] J. D. Brownridge and S. M. Shafroth, "Electron beam production by pyroelectric crystals," in *in Proc. Int. Conf*, Hilton, October 27 – 29, 2002,.

[6] J. A. Geuther and Y. Danon, "Electron and positive ion acceleration with pyroelectric crystals," *J. Appl. Phys,* p. 074109 – 074115, 2005.

[7] V. I. Nagaichenko, et. al., "Electron energy increase in the pyroelectric accelerator," in *Sci. and Tech*, Malmo, 2008.

[8] J. Brownridge and S. Shafroth, "Electron and positive ion beams and x-rays produced by heated and cooled pyroelectric crystals such as LiNbO3 and LiTaO3 in dilute gases: phenomenology and applications.," *Nova Science Publishers,* pp. 57-94, 2005.

[9] J. D. Brownridge and S. M. Shafroth, "Self-focused electron beams produced by pyroelectric crystals on heating or cooling in dilute gases.," *Appl. Phys,* vol. 79, pp. 3364-3366, 2001.

[10] J. D. Brownridge, S. M. Shafroth and D. W. Trott, "Observation of multiple nearly monoenergetic electron production by

pyroelectric crystals in ambient gas.," *Appl. Phys. Lett.,* vol. 78, pp. 1158-1162, 2001.

[11] J. D. Brownridge and S. Raboy, "S. Investigations of pyroelectric generation of x-rays," *J. Appl. Phys.,* vol. 86, pp. 640-643, 1999.

[12] J. D. Brownridge, "Pyroelectric x-ray generator," *Nature,* vol. 358, pp. 277-278, 1992.

[13] J. D. Brownridge, "X-ray fluoresced high-Z (up to Z=82) K x-rays produced by LiNbO3 and LiTaO3 pyroelectric crystal electron accelerators," *Appl. Phys. Lett,* vol. 58, pp. 1298-1304, 2005.

[14] J. Geuther and Y. Danon, "High energy x-ray production with pyroelectric crystals," *J. appl. Phys,* vol. 97, pp. 104916-104921, 2005.

[15] Amptek, "Pyroelectric X-Ray source COOL-X,," [Online]. Available: http://www.amptek.com/pdf/coolx.pdf.

[16] J. Geuther, "Radiation generation with pyroelectric crystals. PhD Thesis," Rensselaer Polytechnic Institute, Troy,, New York, 2007.

[17] N. Kukhtarev. et. al., "Generation of focused electron beam by pyroelectric and photogalvanic crystals.," *Appl. Phys.,* vol. 96, pp. 6794-6798, 2004.

[18] A. N. Oleinik, "Investigation of electrons and X-rays generated by a LiTaO3 single crystal accelerator driven by periodically varying temperature," Royal Holloway University of London, PhD, Thesis. 2021.

[19] P. Karataev, M. Ali, K. Fedorov, A. Kubankin, A. Oleinik and A. Shchagin, "A. Shchagin, Quasi-continuous X-ray generation in LiTaO3-based pyroelectric accelerator driven by periodically varying temperature," *to be publish*..

[20] J. P. Brownridge and S. M. shafroth, Self-focused electron beams produced by pyroelectric crystals on heating or cooling in dilute gases, Appl. Phys., 8 November, 2001..

[21] F. Massines and a. et., "Glow and Townsend dielectric barrier discharge in various," *Plasm. Phys. Control. Fusion,* vol. 47, p. B577, 2005.

[22] A. Stanković,, I. Zlatković, R. Nikolov, B. Brindić and D. Pantić, "Influence of vacuum degassing on microchannel plate performance," Department of Microelectronics, Faculty of Electronic Engineering, University of Niš, Aleksandra Medvedeva 14, 18000 Niš, Serbia, Serbia.

[23] Y. Vallgren, Christina, raisanen, Jyrki, Tikkanen and Pertti, "Outgassing studies of some accelerator materials," CERN THESIS, France, 18 Jun 2019.

[24] J. Geuther, "Radiation generation with pyroelectric crystals, PhD Thesis," Rensselaer Polytechnic Institute, Troy, New York, 2007.

[25] R. Brandenburg, Dielectric barrier discharges: progress on plasma sources and on the understanding of regimes and single filaments., vol. 26, Plasma Sources Sci. Technol, 2017.